Results in Physics 19 (2020) 103701

Contents lists available at ScienceDirect

Results in Physics

journal homepage: www.elsevier.com/locate/rinp

Effective computational schemes for a mathematical model of relativistic electrons arising in the laser thermonuclear fusion

Mostafa M.A. Khater [a,b,*], Mohamed S. Mohamed [c,d], Choonkil Park [e,**], Raghda A.M. Attia [f]

[a] Department of Mathematics, Faculty of Science, Jiangsu University, 212013, Zhenjiang, China
[b] Department of Mathematics, Obour Institutes, 11828, Cairo, Egypt
[c] Department of Mathematics, Faculty of Science, Taif University, P.O. Box 11099, Taif 21944, Saudi Arabia
[d] Department of Mathematics, Faculty of Science, Al-Azher University, Nasr City, Cairo, 11884, Egypt
[e] Research Institute for Natural Sciences, Hanyang University Seoul 04763, South Korea
[f] Department of Basic Science, Higher Technological Institute, 44634, 10th of Ramadan City, Egypt

ARTICLE INFO

MSC:
35E05
35Q51
35Q92

Keywords:
The nonlinear Klein–Fock–Gordon (KFG) equation
Modified Khater (MK) method
Modified Kudryashov (MKud) method

ABSTRACT

This research paper investigates the computational wave solutions of the nonlinear Klein–Fock–Gordon (KFG) equation by applying two effective recent computational schemes. The nonlinear KFG model is a quantized version of the relativistic energy–momentum relation related to the well-known Schrödinger equation. The modified Khater (MK) and modified Kudryashov (MKud) computational schemes are employed to construct novel explicit wave solutions for figuring out novel physical properties of the investigated model. Some solutions are illustrated in some distinct figures. This paper's novelty and originality are discussed by showing the similarity and differences between our paper and other published papers.

1. Introduction

Several researchers in physical phenomena have recently been working on producing a laser–plasma electron with energy greater than obtained from the thermalized electrons [1–3]. This kind of fast electrons' production describes specific complicated physical processes that accelerate electrons to very high energies [4,5]. Examples of such techniques are the resonant absorption of laser radiation in plasma, multi-mode laser fields with stochastic phase perturbations, two – plasmon decay in the quarter's region – critical mass, relativistic electron, induced Raman scattering in plasma coronas, and so on [6–8]. Practically, the laser–plasma is a promising method in which the processing of high-speed electrons such as cathode of an injector with high current pulsed accelerators offers enormous current dose densities ($>$ 106 A/cm^2), a short duration of the injection pulse ($< 10-9$ s), and the high initial energy of the electrons ($>$ 102 keV) [9–11]. In laser thermonuclear fusion, high-speed electrons play a significant part. Just a small volume of the high-energy electron, with less than one percentage of the absorption laser energy in the central field, would cause one-brand retailing and even monumentally lower upward-compression in hydrodynamic systems acceleration and suppression of nuclear fission goals, prevent the required valve from being realized [12–15].

Many laser–plasma electron phenomena have been mathematically derived in many formulated [16–20]. Consequently, the mathematician and physicists have been focusing on studying these phenomena' dynamical and physical behavior through the mathematical view (computational, semi-analytical, and numerical solutions) [21–23]. Additionally, Many computational schemes have been derived to construct many novel traveling solutions that show the models' characterizes [24–27]. These solutions have been using to evaluate the initial and boundary conditions of these models [28,29]. These conditions allow applying the semi-analytical and numerical schemes to these models to assess the approximate solutions and calculate the absolute value of error between the exact and numerical solutions [30–34].

In this research, we study the nonlinear KFG model that is mathematically given by [35–37]:

$$\mathcal{U}_t - \mathcal{U}_{xx} - a\,\mathcal{U} - b\,\mathcal{U}^2 = 0, \qquad (n > 0), \tag{1}$$

where $\mathcal{U}$ describes the dynamical behavior of the relativistic electrons. While a, b, n are arbitrary constants. Using the following transformation $\mathcal{U}(x,t) = \mathcal{V}(\zeta)$, $\zeta = x + \lambda t$ on Eq. (1), yields converting nonlinear partial differential equation (NLPDE) into the next nonlinear ordinary

* Corresponding author at: Department of Mathematics, Faculty of Science, Jiangsu University, 212013, Zhenjiang, China.
** Corresponding author.
E-mail addresses: mostafa.khater2024@yahoo.com (M.M.A. Khater), baak@hanyang.ac.kr (C. Park).

https://doi.org/10.1016/j.rinp.2020.103701
Received 13 November 2020; Received in revised form 30 November 2020; Accepted 4 December 2020
Available online 8 December 2020

differential equation (NLODE)

$$\lambda\,\mathcal{V}' - \mathcal{V}'' - a\,\mathcal{V} - b\,\mathcal{V}^n = 0. \tag{2}$$

Evaluating the balance value of Eq. (2) leads to $\mathcal{V}''\,\&\,\mathcal{V}^n \Rightarrow m = \frac{2}{n-1}$. Thus, we have to use the following transformation $\mathcal{V} = \psi^{\frac{2}{n-1}}$ for Eq. (2) that leads to the following NLODE

$$\frac{2\,\lambda}{n-1}\,\psi^{\frac{3-n}{n-1}}\,\psi' - \frac{6-2\,n}{(n-1)^2}\,\psi^{\frac{4-2\,n}{n-1}}\,\psi'^2 - \frac{2}{n-1}\,\psi^{\frac{3-n}{n-1}}\,\psi'' - a\,\psi^{\frac{2}{n-1}} - b\,\psi^{\frac{2\,n}{n-1}} = 0. \tag{3}$$

Multiplying Eq. (3) by $\psi^{-\frac{4-2\,n}{n-1}}$, gives

$$\frac{2}{n-1}\,\psi\,\psi' - \frac{6-2\,n}{(n-1)^2}\,\psi'^2 - \frac{2}{n-1}\,\psi\,\psi'' - a\,\psi^2 - b\,\psi^4 = 0. \tag{4}$$

Balancing the highest order and nonlinear terms of Eq. (4), gives $\psi\,\psi''\,\&\,\psi^4 \Rightarrow m = 1$.

The rest sections in this manuscript are organized as follows: Section 2 applies MK and GKud schemes to the nonlinear KFG model for constructing novel solitary solutions [38–41]. Section 3 demonstrates the obtained solutions and their physical interpretations through shown two, three-dimensional, and contour plots. Section 4 gives the conclusion of the whole research paper.

2. Computational wave solutions

Here, we apply two recent analytical schemes (the MK, and GK techniques) to the nonlinear KFG equation for evaluating novel solitary wave solutions

2.1. The MK method

Handling Eq. (4) through the MK analytical technique and the homogeneous balance principles, formulates its general solution in the following form:

$$\psi(\zeta) = \sum_{i=1}^{m} a_i\,\mathcal{K}^{i\,\mathcal{F}(\xi)} + \sum_{j=1}^{m} b_i\,\mathcal{K}^{-j\,\mathcal{F}(\zeta)} + a_0 = a_1\,\mathcal{K}^{\mathcal{F}(\zeta)} + a_0 + b_1\,\mathcal{K}^{-\mathcal{F}(\zeta)}, \tag{5}$$

where $\mathcal{F}(\zeta)$ is the solution function of $\mathcal{F}'(\zeta) = \frac{1}{\ln(\mathcal{K})}\left[\delta + \rho\,\mathcal{K}^{\mathcal{F}(\zeta)} + \varkappa\,\mathcal{K}^{-\mathcal{F}(\zeta)}\right]$ and a_0, a_1, b_1, δ, ρ, $\varkappa$ are arbitrary constants to be determined later. Applying the well-known steps of the Mk method with Eq. (5) through its auxiliary equation to Eq. (4), gives the following families of the above-mentioned parameters:

Family I

$$a_1 \to \frac{a_0\left(\sqrt{\delta^2-4\rho\varkappa}+\delta\right)}{2\varkappa}, b_1 \to 0, \lambda \to 3\sqrt{\delta^2-4\rho\varkappa}, a \to 2\left(\delta^2-4\rho\varkappa\right),$$
$$b \to \frac{\delta\left(\sqrt{\delta^2-4\rho\varkappa}-\delta\right)+2\rho\varkappa}{a_0^2}, n \to 3.$$

Family II

$$a_1 \to 0, b_1 \to \frac{a_0\left(\delta-\sqrt{\delta^2-4\rho\varkappa}\right)}{2\rho}, \lambda \to 3\sqrt{\delta^2-4\rho\varkappa}, a \to 2\left(\delta^2-4\rho\varkappa\right),$$
$$b \to \frac{2\rho\varkappa-\delta\left(\sqrt{\delta^2-4\rho\varkappa}+\delta\right)}{a_0^2}, n \to 3.$$

Thus, many distinct wave solutions Eq. (1) are constructed in the following form:

For $\delta^2 - 4\rho\varkappa > 0$, $\rho \neq 0$, the explicit solution is given by

$$\mathcal{U}_{I,1}(x,t) = -\frac{a_0\left(\delta\left(\sqrt{\delta^2-4\rho\varkappa}+\delta\right)-4\rho\varkappa\right)\left(\tanh\left(\frac{1}{2}\left(3t\left(\delta^2-4\rho\varkappa\right)+x\sqrt{\delta^2-4\rho\varkappa}\right)\right)+1\right)}{4\rho\varkappa}, \tag{6}$$

$$\mathcal{U}_{I,2}(x,t) = -\frac{a_0\left(\delta\left(\sqrt{\delta^2-4\rho\varkappa}+\delta\right)-4\rho\varkappa\right)\left(\coth\left(\frac{1}{2}\left(3t\left(\delta^2-4\rho\varkappa\right)+x\sqrt{\delta^2-4\rho\varkappa}\right)\right)+1\right)}{4\rho\varkappa}, \tag{7}$$

$$\mathcal{U}_{II,1}(x,t) = \frac{a_0\sqrt{\delta^2-4\rho\varkappa}\left(\tanh\left(\frac{1}{2}\left(3t\left(\delta^2-4\rho\varkappa\right)+x\sqrt{\delta^2-4\rho\varkappa}\right)\right)+1\right)}{\delta+\sqrt{\delta^2-4\rho\varkappa}\tanh\left(\frac{1}{2}\left(3t\left(\delta^2-4\rho\varkappa\right)+x\sqrt{\delta^2-4\rho\varkappa}\right)\right)}, \tag{8}$$

$$\mathcal{U}_{II,2}(x,t) = \frac{a_0\sqrt{\delta^2-4\rho\varkappa}\left(\coth\left(\frac{1}{2}\left(3t\left(\delta^2-4\rho\varkappa\right)+x\sqrt{\delta^2-4\rho\varkappa}\right)\right)+1\right)}{\delta+\sqrt{\delta^2-4\rho\varkappa}\coth\left(\frac{1}{2}\left(3t\left(\delta^2-4\rho\varkappa\right)+x\sqrt{\delta^2-4\rho\varkappa}\right)\right)}. \tag{9}$$

For $\rho\varkappa < 0$, $\rho \neq 0$, $\varkappa \neq 0$, $\delta = 0$, the explicit solution is given by

$$\mathcal{U}_{I,3}(x,t) = -a_0\left(\tanh\left(6\rho t\varkappa - x\sqrt{\rho(-\varkappa)}\right)-1\right), \tag{10}$$

$$\mathcal{U}_{I,4}(x,t) = a_0\left(-\left(\coth\left(6\rho t\varkappa - x\sqrt{\rho(-\varkappa)}\right)-1\right)\right), \tag{11}$$

$$\mathcal{U}_{II,3}(x,t) = a_0\left(-\left(\coth\left(6\rho t\varkappa - x\sqrt{\rho(-\varkappa)}\right)-1\right)\right), \tag{12}$$

$$\mathcal{U}_{II,4}(x,t) = -a_0\left(\tanh\left(6\rho t\varkappa - x\sqrt{\rho(-\varkappa)}\right)-1\right). \tag{13}$$

For $\delta = 0$, $\varkappa = -\rho$, the explicit solution is given by

$$\mathcal{U}_{I,5}(x,t) = \frac{a_0\left(\sqrt{\varkappa^2}\coth\left(\varkappa\left(6t\sqrt{\varkappa^2}+x\right)\right)+\varkappa\right)}{\varkappa}, \tag{14}$$

$$\mathcal{U}_{II,5}(x,t) = \frac{a_0\left(\sqrt{\varkappa^2}\tanh\left(\varkappa\left(6t\sqrt{\varkappa^2}+x\right)\right)+\varkappa\right)}{\varkappa}. \tag{15}$$

For $\delta = \frac{\varkappa}{2} = \kappa$, $\rho = 0$, the explicit solution is given by

$$\mathcal{U}_{I,6}(x,t) = \frac{1}{4}a_0\left(\frac{\left(\sqrt{\kappa^2}+\kappa\right)\left(e^{\kappa\left(3\sqrt{\kappa^2}t+x\right)}-2\right)}{\kappa}+4\right). \tag{16}$$

For $\delta = \rho = \kappa$, $\varkappa = 0$, the explicit solution is given by

$$\mathcal{U}_{II,6}(x,t) = \frac{a_0\left(\sqrt{\kappa^2}+\kappa+\left(\kappa-\sqrt{\kappa^2}\right)e^{-\kappa\left(3\sqrt{\kappa^2}t+x\right)}\right)}{2\kappa}. \tag{17}$$

For $\rho = 0$, $\delta \neq 0$, $\varkappa \neq 0$, the explicit solution is given by

$$\mathcal{U}_{I,7}(x,t) = \frac{1}{2}a_0\left(\frac{\left(\sqrt{\delta^2}+\delta\right)\left(e^{\delta\left(3\sqrt{\delta^2}t+x\right)}-\frac{\varkappa}{\delta}\right)}{\varkappa}+2\right). \tag{18}$$

For $\varkappa = 0$, $\delta \neq 0$, $\rho \neq 0$, the explicit solution is given by

$$\mathcal{U}_{II,7}(x,t) = \frac{a_0\left(\sqrt{\delta^2}+\delta-\frac{2\left(\sqrt{\delta^2}-\delta\right)e^{-\delta\left(3\sqrt{\delta^2}t+x\right)}}{\rho}\right)}{2\delta}. \tag{19}$$

2.2. The MKud method

Handling Eq. (4) through the MKud analytical technique and the homogeneous balance principles, formulates its general solution in the following form:

$$\psi(\zeta) = \sum_{i=0}^{m} a_i\mathcal{Q}(\zeta)^i = a_1\,\mathcal{Q}(\zeta) + a_0, \tag{20}$$

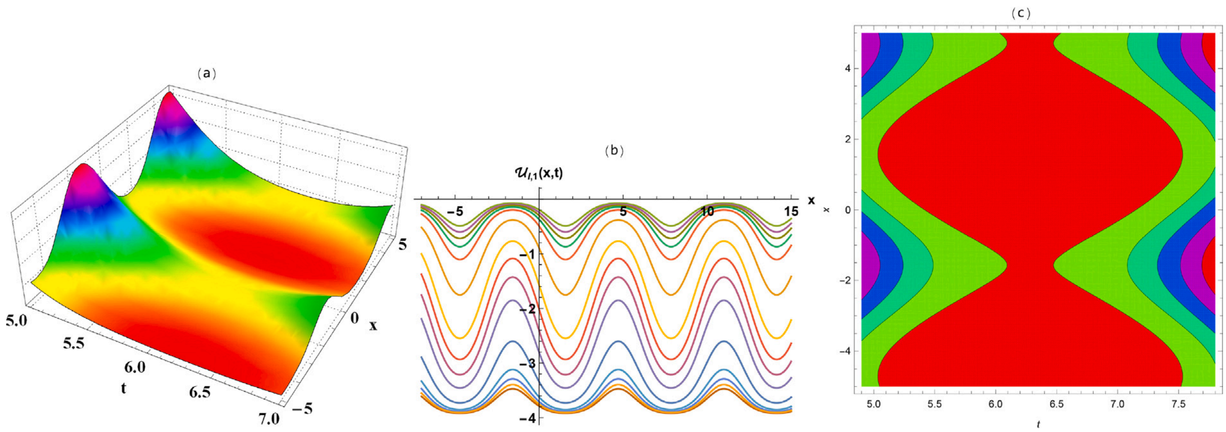

Fig. 1. Three distinct types of numerical sketches ((a) 3D, (b) 2D, and (c) contour plots) of Eq. (6).

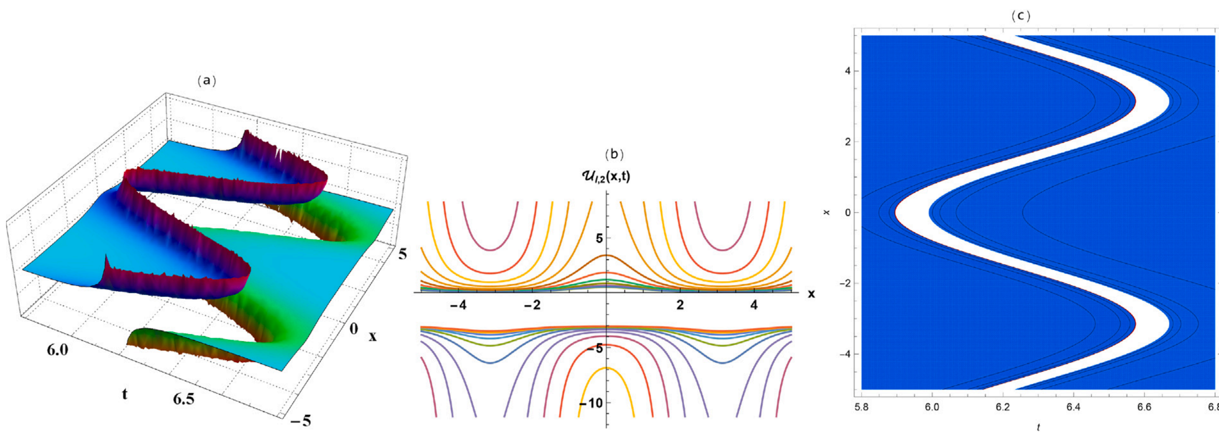

Fig. 2. Three different types of numerical sketches ((a) 3D, (b) 2D, and (c) contour plots) of Eq. (7).

where $\mathcal{Q}(\zeta)$ is the solution function of $\mathcal{Q}'(\zeta) \to (\mathcal{Q}(\zeta)^2 - \mathcal{Q}(\zeta))\log(r)$ and a_0, a_1, r are arbitrary constants to be evaluated later.

Family I

$$a_0 \to 0, \lambda \to \frac{-n\log(r) - 3\log(r)}{n-1}, a \to \frac{2(n+1)\log^2(r)}{(n-1)^2},$$
$$b \to -\frac{2(n+1)\log^2(r)}{a_1^2(n-1)^2}.$$

Family II

$$a_0 \to -a_1, \lambda \to \frac{(n+3)\log(r)}{n-1}, a \to \frac{2(n+1)\log^2(r)}{(n-1)^2}, b \to -\frac{2(n+1)\log^2(r)}{a_1^2(n-1)^2}.$$

Family III

$$a_0 \to -a_1, \lambda \to 3\log(r), n \to 3, a \to 2\log^2(r), b \to -\frac{2\log^2(r)}{a_1^2}.$$

Thus, many distinct wave solutions Eq. (1) are constructed in the following form:

$$\mathcal{U}_1(x,t) = \left(\frac{a_1}{1 \pm r^{\frac{t(-n\log(r)-3\log(r))}{n-1}+x}}\right)^{\frac{2}{n-1}}, \tag{21}$$

$$\mathcal{U}_2(x,t) = \left(a_1\left(\frac{1}{1 \pm r^{\frac{(n+3)t\log(r)}{n-1}+x}} - 1\right)\right)^{\frac{2}{n-1}}, \tag{22}$$

$$\mathcal{U}_3(x,t) = a_1\left(\frac{1}{1 \pm r^{3t\log(r)+x}} - 1\right). \tag{23}$$

3. Results and discussion

Here, the employed and constructed solutions are discussed and explained to show the novelty and originality of the obtained solutions and whole research paper. This discussion-based on comparing both used schemes and their results. Moreover, It also reaches to demonstrate the shown figures and their physical interpretation (Figs. 1–7).

1. ***The computational used scheme***:
   The MK and GK techniques have been used as the first time for the nonlinear KFG model. These schemes are equal under the following conditions $\mathcal{K}^{\mathcal{F}(\zeta)} = \mathcal{Q}(\zeta)$, $\mathcal{K} = r$, $\rho = -\delta = 1$, $\varkappa = 0$. However, this equivalence between both methods but the MK method has obtained solutions more than GK method. The MK method also has covered the obtained solutions that have been obtained by the GK method.
2. ***The obtained solutions***:
   Here, we compare our solutions and that have been obtained by A. N. Bulygin, Yu. V. Pavlov & Eron L. Aero, A. N. Bulygin, Yu. V. Pavlov in [42,43] where they have employed the principles of construction of functionally to study the nonlinear KFG equation. They have evaluated many various solutions of the investigated model however our paper contains more than their constructed solutions.
3. ***The physical explanation of the shown figures:***
   The solutions of the KFG model are represented in some distinct figures to show novel properties of dynamical behavior of the relativistic electrons. Eqs. (6), (7), (8), (9), (21), (22), and (23)

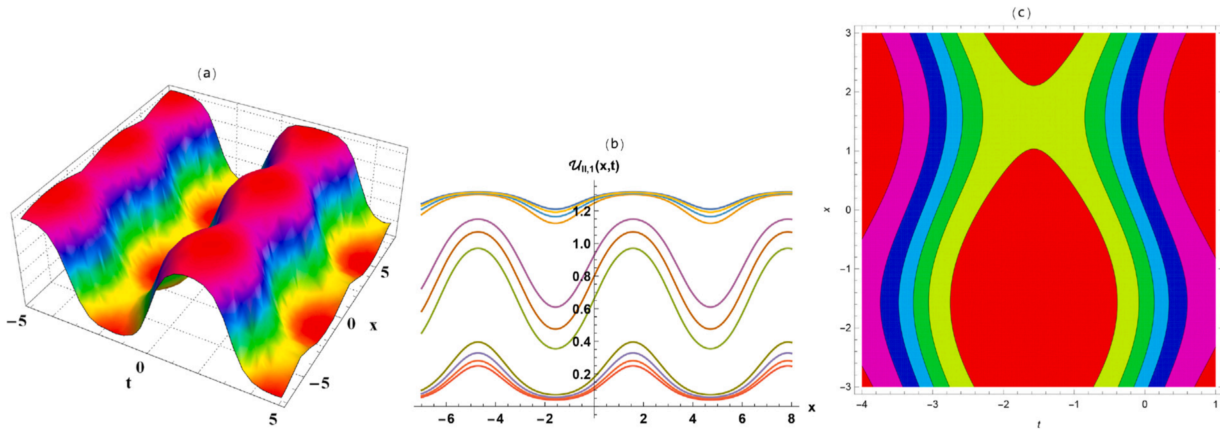

Fig. 3. Three various types of numerical sketches ((a) 3D, (b) 2D, and (c) contour plots) of Eq. (8).

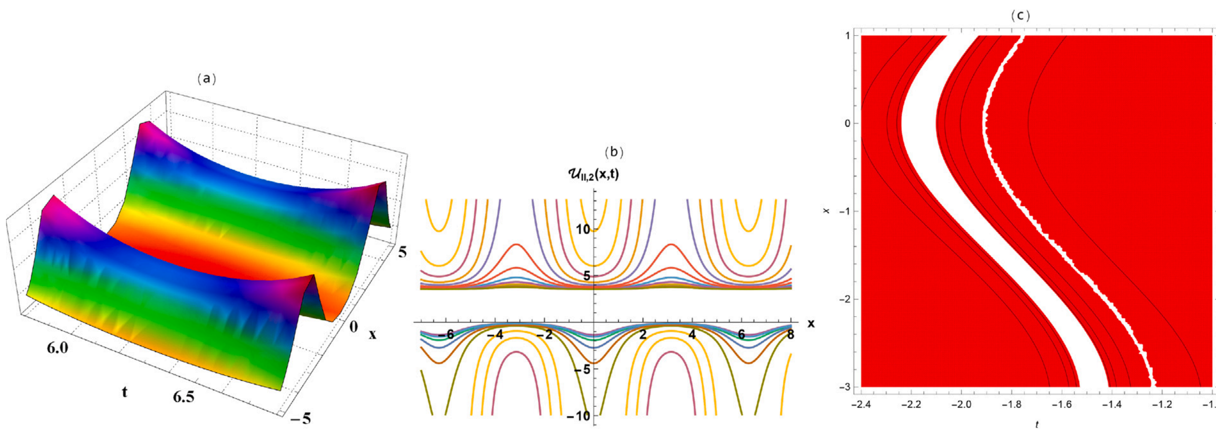

Fig. 4. Three distinct types of numerical sketches ((a) 3D, (b) 2D, and (c) contour plots) of Eq. (9).

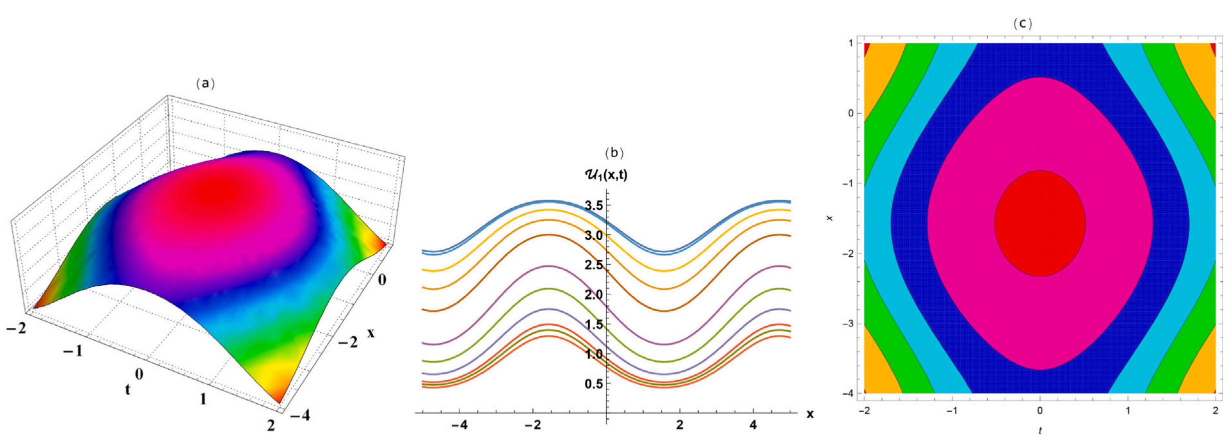

Fig. 5. Three distinct types of numerical sketches ((a) 3D, (b) 2D, and (c) contour plots) of Eq. (21).

are sketched in three, two-dimensional and contour plots with the following numerical values of the parameters $\left[a_0 = 4, \delta = 3, \rho = 1, \varkappa = 2 \,\&\, a_0 = 6, \delta = 5, \rho = 3, \varkappa = 2 \,\&\, a_0 = 4, \delta = 5, \rho = 2, \varkappa = 3 \,\&\, a_0 = 7, \delta = 3, \rho = 2, \varkappa = 1 \,\&\, a_1 = 4, n = 3, r = 2 \,\&\, a_1 = 5, n = 3, r = 4 \,\&\, a_1 = 6, r = 7\right]$. These Figs. 1, 2, 3, 4, 5, 6, 7 show respectively breath, solitary, periodic, breath, cone, kink, and anti-kink shapes that explain the model's physical characterizes.

4. Conclusion

In this manuscript, novel solitary wave solutions of the nonlinear KFG model have productively constructed. The MK and MKud computational schemes and homogeneous balance principles have been successfully applied to the nonlinear ordinary differential equation that have been obtained by employing the wave transformation for the original nonlinear partial differential equation of the KFG model. Some solutions have been sketched in three distinct types of figures and showed novel physical properties of the studied model. The originality of this paper has been discussed and demonstrated by comparing

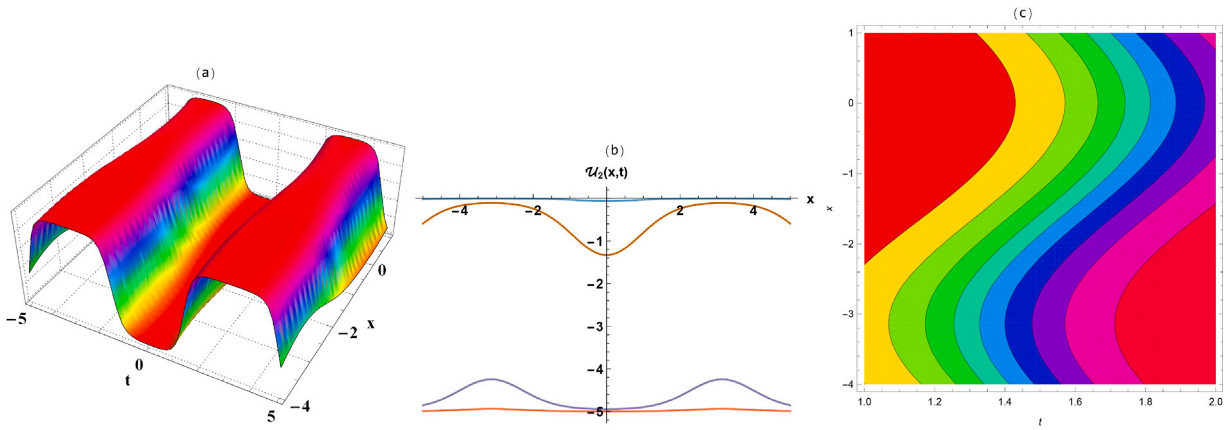

Fig. 6. Three different types of numerical sketches ((a) 3D, (b) 2D, and (c) contour plots) of Eq. (22).

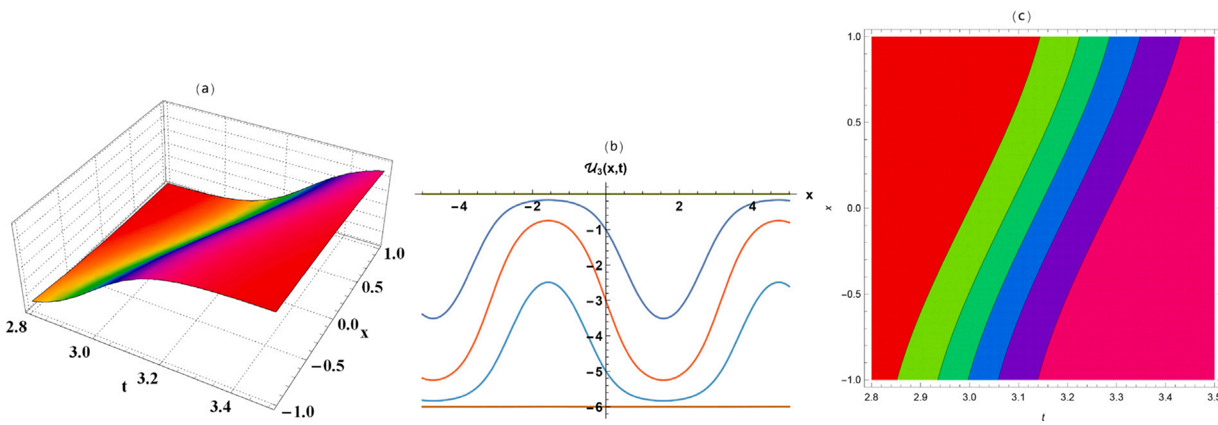

Fig. 7. Three various types of numerical sketches ((a) 3D, (b) 2D, and (c) contour plots) of Eq. (23).

the used schemes together and showing the difference between our solutions and that have been obtained in previously published paper. The performance of both used schemes shows their effective and ability for handling many nonlinear evolution equation in integer or fractional order.

Declaration of competing interest

The authors declare that they have no known competing financial interests or personal relationships that could have appeared to influence the work reported in this paper.

Data availability statement

The data that support the findings of this study are available from the corresponding author upon reasonable request.

Acknowledgment

The work was supported by Taif University researchers Supporting Project number (TURSP-2020/160), Taif University, Taif, Saudi Arabia.

Fund

This paper was funded from by Taif University researchers Supporting Project number (TURSP-2020/160), Taif University, Taif, Saudi Arabia.

References

[1] Lumpkin A, LaBerge M, Rule D, Zgadzaj R, Hannasch A, Zarini O, et al. Coherent optical signatures of electron microbunching in laser-driven plasma accelerators. Phys Rev Lett 2020;125(1):014801.
[2] Gleixner F, Kumar N. Electronic parametric instabilities of an ultrarelativistic laser pulse in a plasma. Phys Rev E 2020;101(3):033201.
[3] Atangana A, Akgül A. Can transfer function and bode diagram be obtained from sumudu transform. Alexandria Eng J 2020.
[4] Li G, Ain Q, Li S, Saeed M, Papp D, Kamperidis C, et al. Control of electron beam energy-spread by beam loading effects in a laser-plasma accelerator. Plasma Phys Control Fusion 2020;62(5):055004.
[5] Owolabi KM, Atangana A, Akgul A. Modelling and analysis of fractal-fractional partial differential equations: Application to reaction-diffusion model. Alexandria Eng J 2020.
[6] Maier A, Kajumba N, Guggenmos A, Werle C, Wenz J, Delbos N, et al. Water-window X-Ray pulses from a laser-plasma driven undulator. Sci Rep 2020;10(1):1–8.
[7] Tajima T, Malka V. Laser plasma accelerators. Plasma Phys Control Fusion 2020;62(3):034004.
[8] Atangana A, Akgül A, Owolabi KM. Analysis of fractal fractional differential equations. Alexandria Eng J 2020.
[9] Zhu C-q, Wang J-g, Li Y-f, Feng J, Li D-z, He Y-h, et al. Optical steering of electron beam in laser plasma accelerators. Opt Express 2020;28(8):11609–17.
[10] Zhu X-L, Chen M, Weng S-M, Yu T-P, Wang W-M, He F, et al. Extremely brilliant gev γ-rays from a two-stage laser-plasma accelerator. Sci Adv 2020;6(22):eaaz7240.
[11] Atangana A, Akgül A. On solutions of fractal fractional differential equations. Discrete Contin Dyn Syst S 2018.
[12] Cao S, Yan R, Wen H, Li J, Ren C. Cogeneration of hot electrons from multiple laser-plasma instabilities. Phys Rev E 2020;101(5):053205.
[13] Akgül A. A novel method for a fractional derivative with non-local and non-singular kernel. Chaos Solitons Fractals 2018;114:478–82.
[14] Wakif A, Boulahia Z, Sehaqui R. A semi-analytical analysis of electro-thermo-hydrodynamic stability in dielectric nanofluids using buongiorno's mathematical model together with more realistic boundary conditions. Results Phys 2018;9:1438–54.

[15] Wakif A, Boulahia Z, Sehaqui R. Numerical analysis of the onset of longitudinal convective rolls in a porous medium saturated by an electrically conducting nanofluid in the presence of an external magnetic field. Results Phys 2017;7:2134–52.
[16] El-Monier S, Atteya A. Dynamics of ion-acoustic waves in nonrelativistic magnetized multi-ion quantum plasma: the role of trapped electrons. Waves Random Complex Media 2020;1–19.
[17] Feng Y, Hou L. The solitary wave solution for quantum plasma nonlinear dynamic model. Adv Math Phys 2020;2020.
[18] Ali KK, Yilmazer R, Baskonus H, Bulut H. Modulation instability analysis and analytical solutions to the system of equations for the ion sound and Langmuir waves. Phys Scr 2020;95(6):065602.
[19] Zaydan M, Wakif A, Animasaun I, Khan U, Baleanu D, Sehaqui R. Significances of blowing and suction processes on the occurrence of thermo-magneto-convection phenomenon in a narrow nanofluidic medium: A revised buongiorno's nanofluid model. Case Stud Therm Eng 2020;22:100726.
[20] Wakif A, Chamkha A, Thumma T, Animasaun I, Sehaqui R. Thermal radiation and surface roughness effects on the thermo-magneto-hydrodynamic stability of alumina–copper oxide hybrid nanofluids utilizing the generalized buongiorno's nanofluid model. J Therm Anal Calorim 2020;1–20.
[21] El-Monier S, Atteya A. Dynamics of ion-acoustic waves in nonrelativistic magnetized multi-ion quantum plasma: the role of trapped electrons. Waves Random Complex Media 2020;1–19.
[22] Feng Y, Hou L. The solitary wave solution for quantum plasma nonlinear dynamic model. Adv Math Phys 2020;2020.
[23] Wakif A, Boulahia Z, Ali F, Eid MR, Sehaqui R. Numerical analysis of the unsteady natural convection mhd couette nanofluid flow in the presence of thermal radiation using single and two-phase nanofluid models for cu–water nanofluids. Int J Appl Comput Math 2018;4(3):81.
[24] Yang C, Rodriguez N. A numerical perspective on traveling wave solutions in a system for rioting activity. Appl Math Comput 2020;364:124646.
[25] Khater MM, Lu D, Zahran EH. Solitary wave solutions of the benjamin–bona–mahoney–Burgers equation with dual power-law nonlinearity. Appl Math Inf Sci 2017;11(5):1–5.
[26] Lu D, Seadawy AR, Khater MM. Dispersive optical soliton solutions of the generalized radhakrishnan–kundu–lakshmanan dynamical equation with power law nonlinearity and its applications. Optik 2018;164:54–64.
[27] Wakif A, Boulahia Z, Mishra S, Rashidi MM, Sehaqui R. Influence of a uniform transverse magnetic field on the thermo-hydrodynamic stability in water-based nanofluids with metallic nanoparticles using the generalized buongiorno's mathematical model. Eur Phys J Plus 2018;133(5):181.
[28] Liu J-G, Yang X-J, Feng Y-Y. Characteristic of the algebraic traveling wave solutions for two extended (2+ 1)-dimensional kadomtsev–petviashvili equations. Modern Phys Lett A 2020;35(07):2050028.
[29] Lu D, Seadawy AR, Khater MM. Structures of exact and solitary optical solutions for the higher-order nonlinear Schrödinger equation and its applications in mono-mode optical fibers. Modern Phys Lett B 2019;33(23):1950279.
[30] Seadawy AR, Lu D, Khater MM. Bifurcations of solitary wave solutions for the three dimensional Zakharov–Kuznetsov–Burgers equation and Boussinesq equation with dual dispersion. Optik 2017;143:104–14.
[31] Park C, Khater MM, Attia RA, Alharbi W, Alodhaibi SS. An explicit plethora of solution for the fractional nonlinear model of the low–pass electrical transmission lines via Atangana–Baleanu derivative operator. Alexandria Eng J 2020.
[32] Yue C, Khater MM, Attia RA, Lu D. The plethora of explicit solutions of the fractional KS equation through liquid–gas bubbles mix under the thermodynamic conditions via Atangana–Baleanu derivative operator. Adv Difference Equ 2020;2020(1):1–12.
[33] Khater MM, Attia RA, Lu D. Computational and numerical simulations for the nonlinear fractional Kolmogorov–Petrovskii–Piskunov (FKPP) equation. Phys Scr 2020;95(5):055213.
[34] Abdel-Aty A-H, Khater MM, Attia R, Abdel-Aty M, Eleuch H. On the new explicit solutions of the fractional nonlinear space-time nuclear model. Fractals 2020;28(8):2040035.
[35] Bulygin AN, Pavlov YV. Solutions of nonlinear nonautonomous Klein–Fock–Gordon equation. The choice of ansatz. In: 2019 days on diffraction (DD). IEEE; 2019, p. 22–6.
[36] Bulygin A, Pavlov YV. New ansatzes for solution of nonlinear nonautonomous Klein-Fock-Gordon equation. In: International summer school-conference "advanced problems in mechanics". Springer; 2019, p. 72–80.
[37] Veeresha P, Prakasha DG, Kumar D. An efficient technique for nonlinear time-fractional Klein–Fock–Gordon equation. Appl Math Comput 2020;364:124637.
[38] Khater MM, Attia RA, Abdel-Aty A-H, Abdou M, Eleuch H, Lu D. Analytical and semi-analytical ample solutions of the higher-order nonlinear Schrödinger equation with the non-Kerr nonlinear term. Results Phys 2020;16:103000.
[39] Ali AT, Khater MM, Attia RA, Abdel-Aty A-H, Lu D. Abundant numerical and analytical solutions of the generalized formula of Hirota-Satsuma coupled KdV system. Chaos Solitons Fractals 2020;131:109473.
[40] Hyder A-A. White noise theory and general improved kudryashov method for stochastic nonlinear evolution equations with conformable derivatives. Adv Difference Equ 2020;2020(1):1–19.
[41] Hyder A-A, Barakat M. General improved kudryashov method for exact solutions of nonlinear evolution equations in mathematical physics. Phys Scr 2020;95(4):045212.
[42] Bulygin A, Pavlov YV. Methods of finding of exact analytical solutions of nonautonomous nonlinear Klein-Fock-Gordon equation. In: Dynamical processes in generalized continua and structures. Springer; 2019, p. 147–61.
[43] Aero EL, Bulygin A, Pavlov YV. Exact analytical solutions for nonautonomic nonlinear Klein-Fock-Gordon equation. In: Advances in mechanics of microstructured media and structures. Springer; 2018, p. 21–33.